

RESEARCH LETTER

10.1002/2014GL062069

Key Points:

- Three terms balance at the transition between dipolar and multipolar dynamos
- A unique parameter accurately describes this balance in numerical models
- Dipolar models involve viscosity as opposed to expectation for the geodynamo

Correspondence to:

E. Dormy,  
dormy@phys.ens.fr

Citation:

Oruba, L., and E. Dormy (2014), Transition between viscous dipolar and inertial multipolar dynamos, *Geophys. Res. Lett.*, *41*, doi:10.1002/2014GL062069.

Received 30 SEP 2014

Accepted 1 OCT 2014

Accepted article online 2 OCT 2014

## Transition between viscous dipolar and inertial multipolar dynamos

Ludvine Oruba<sup>1</sup> and Emmanuel Dormy<sup>1,2</sup>

<sup>1</sup>MAG (ENS/IPGP) LRA, Département de Physique, Ecole Normale Supérieure, Paris, France, <sup>2</sup>Institut de Physique du Globe de Paris, CNRS/UMR7154, Paris, France

**Abstract** We investigate the transition from steady dipolar to reversing multipolar dynamos. The Earth has been argued to lie close to this transition, which could offer a scenario for geomagnetic reversals. We show that the transition between dipolar and multipolar dynamos is characterized by a three terms balance (as opposed to the usually assumed two terms balance), which involves the nongradient parts of inertial, viscous and Coriolis forces. We introduce from this equilibrium the sole parameter  $Ro E^{-1/3} \equiv Re E^{2/3}$ , which accurately describes the transition for a wide database of 132 fully three-dimensional direct numerical simulations of spherical rotating dynamos (courtesy of U. Christensen). This resolves earlier contradictions in the literature on the relevant two terms balance at the transition. Considering only a two terms balance between the nongradient part of the Coriolis force and of inertial forces provides the classical  $Ro/\ell_v$ . This transition can be equivalently described by  $Re \ell_v^2$ , which corresponds to the two terms balance between the nongradient part of inertial forces and viscous forces.

### 1. Introduction

The transition between the dipolar dynamo regime and a nondipolar regime was first pointed out by *Kuzner and Christensen* [2002]. They observed through direct numerical experiments two different regimes of dynamo action. One, at moderate forcing, characterized by a steady large-scale dipole and the other, with a more vigorous forcing, revealing multipolar solutions and chaotic reversals of the dipolar component. The existence of these two regimes and their possible relevance to the geodynamo is a central problem in geomagnetism.

*Christensen and Aubert* [2006] found through a wide parameter space survey that this transition is controlled by the relative strengths of inertial and Coriolis forces, as measured by the so-called “local Rossby number.” More recently, *Soderlund et al.* [2012] argued that the Coriolis force was dominant in both regimes and suggested, instead, that the transition was controlled by the relative strengths of inertial to viscous forces, both of lower amplitude.

In this letter, we use a wide database of 132 fully three-dimensional direct numerical simulations (kindly provided by U. Christensen) to address this apparent contradiction. We argue that both interpretations are in fact equivalent if one considers the nongradient part of the forces balance only. This is easily achieved by considering the curl of the relevant forces. The fluid being incompressible, the gradient part of any force will obviously be balanced by pressure forces.

### 2. Modeling

Our study relies on a database of numerical simulations performed in a spherical shell of typical width  $L = r_o - r_i$  and aspect ratio  $\xi \equiv r_i/r_o = 0.35$ . The flow is thermally driven by an imposed difference of temperature between the inner and outer spheres. These simulations rely on no-slip mechanical boundary conditions and an insulating outer domain. Most of simulations involve an insulating inner core, a few of them involve a conducting inner core with the same conductivity as the fluid.

The governing equations in the rotating reference frame can then be written in their nondimensional form—using  $L$  as unit of length,  $(2\Omega)^{-1}$  as unit of time,  $\Delta T$  as unit of temperature, and  $2\Omega \sqrt{\rho\mu} L$  as unit for the magnetic field—as

$$\partial_t \mathbf{u} + (\mathbf{u} \cdot \nabla) \mathbf{u} = -\nabla \pi + E \Delta \mathbf{u} - \mathbf{e}_z \times \mathbf{u} + \frac{Ra E^2}{Pr} T \frac{\mathbf{r}}{r_o} + (\nabla \times \mathbf{B}) \times \mathbf{B}, \quad (1)$$

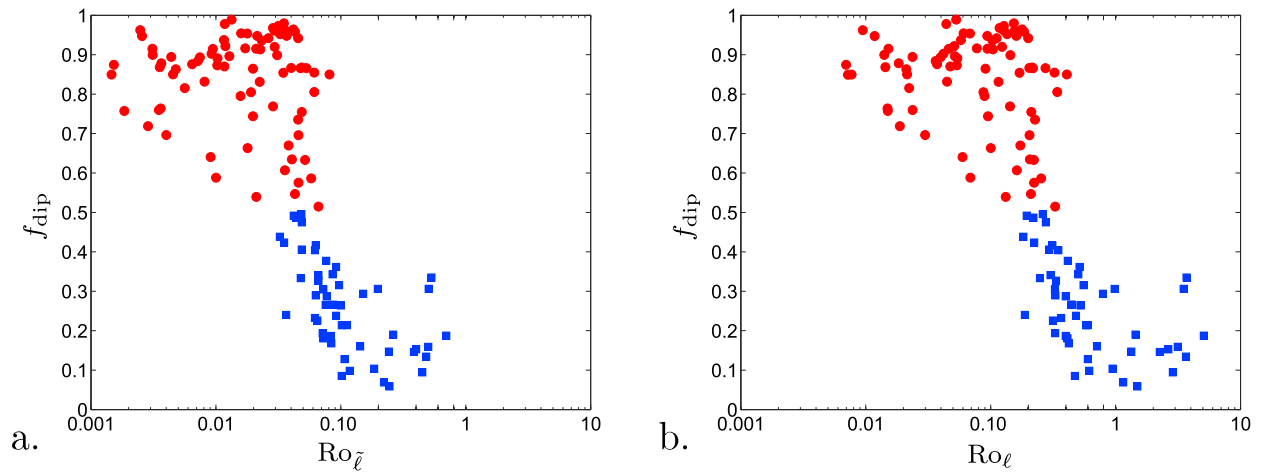


**Figure 1.** Dipolarity as measured by  $f_{\text{dip}}$  versus (a) the local Rossby number  $Ro_{\tilde{\ell}}$  as defined by *Christensen and Aubert* [2006] (b) the local Rossby number  $Ro_{\ell}$  as defined by *Oruba and Dormy* [2014]. Red circles (respectively, blue squares) correspond to  $f_{\text{dip}} > 0.5$  (respectively,  $f_{\text{dip}} < 0.5$ ). These graphs rely on the 132 dynamos database.

$$\partial_t \mathbf{B} = \nabla \times (\mathbf{u} \times \mathbf{B}) + \frac{E}{Pm} \Delta \mathbf{B}, \quad \partial_t T + (\mathbf{u} \cdot \nabla) T = \frac{E}{Pr} \Delta T, \quad (2)$$

$$\nabla \cdot \mathbf{u} = \nabla \cdot \mathbf{B} = 0. \quad (3)$$

These equations involve four nondimensional numbers: the Ekman number  $E = \nu / (2\Omega L^2)$ , the Prandtl number  $Pr = \nu / \kappa$ , the magnetic Prandtl number  $Pm = \nu / \eta$ , and the Rayleigh number  $Ra = \alpha g_0 \Delta T L^3 / (\nu \kappa)$ , in which  $\nu$  is the kinematic viscosity of the fluid,  $\alpha$  the coefficient of thermal expansion,  $g_0$  the gravity at the outer bounding sphere,  $\kappa$  its thermal diffusivity, and  $\eta$  its magnetic diffusivity.

The database used for this study covers the parameter range  $E \in [5 \times 10^{-7}, 5 \times 10^{-4}]$  and  $Pm \in [0.04, 33.3]$  and is restricted to  $Pr = 1$ . We therefore cannot distinguish any possible dependence on the Prandtl number  $Pr$  from our analysis.

### 3. Coriolis Versus Inertial Forces

The dipolarity of the magnetic field is well quantified by  $f_{\text{dip}}$ , which corresponds to the time-averaged ratio of the mean dipole field strength to the field strength in harmonic degrees  $n = 1 - 12$  at the outer bounding sphere [see *Christensen and Aubert*, 2006]. We also introduce the Rossby number  $Ro$ , defined using time-averaged quantities as

$$Ro \equiv \langle \mathbf{u}^2 \rangle^{1/2} \equiv u, \quad (4)$$

where  $\langle \cdot \rangle$  denotes the volume average over the shell. *Christensen and Aubert* [2006] empirically show that the transition from the dipolar regime to the nondipolar regime occurs at  $Ro_{\tilde{\ell}} \simeq 0.1$  (which becomes  $Ro_{\tilde{\ell}} \simeq 0.05$  with our definition of the time scale), where  $Ro_{\tilde{\ell}}$  denotes the local Rossby number, defined as  $Ro_{\tilde{\ell}} = Ro / \tilde{\ell}_u$ . This transition was also shown to work with stress-free boundary conditions [*Schrinner et al.*, 2012]. The typical length scale of the flow  $\tilde{\ell}_u$  is here defined as  $\pi / \bar{n}$ , where  $\bar{n}$  corresponds to the mean value of the spherical harmonics degree  $n$  in the time-averaged kinetic energy spectrum [see *Christensen and Aubert*, 2006, equation (27)]. Figure 1a represents the dipolarity  $f_{\text{dip}}$  as a function of  $Ro_{\tilde{\ell}}$ , when applied to the 132 dynamos database.

The above definition of  $\tilde{\ell}_u$  is anisotropic as it does not take the radial variations into account. Indeed, it only involves the spherical harmonics degree  $n$  of the spectral decomposition. Moreover, this calculus relies on a radial averaging: the role of the radius  $r$  in the length scale associated to a given angular scale is thus not taken into account. *Oruba and Dormy* [2014] introduced the kinematic dissipation length scale, denoted here as  $\ell_u$ , defined using time-averaged quantities as

$$\ell_u^2 \equiv \frac{\langle \mathbf{u}^2 \rangle}{\langle (\nabla \times \mathbf{u})^2 \rangle}. \quad (5)$$

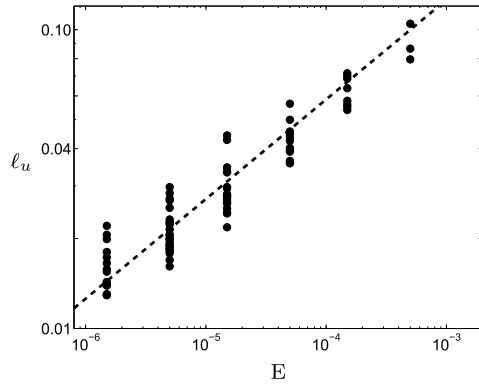


**Figure 2.** The nondimensional characteristic length scale  $\ell_u$  as a function of the Ekman number. The dashed line corresponds to  $\ell_u \sim E^{1/3}$ . This plot relies on a subset of 81 dynamos, corresponding to  $f_{\text{dip}} > 0.5$ .

Contrary to  $\tilde{\ell}_u$ , this length scale  $\ell_u$  is isotropic. Using the 132 dynamos database, the two length scales are found roughly proportional, with  $\tilde{\ell}_u \simeq 5\ell_u$ : as expected  $\tilde{\ell}_u > \ell_u$ . We can then introduce the local Rossby number  $Ro_\ell$ , defined as  $Ro_\ell = Ro/\ell_u$ . The transition between the dipolar regime and the multipolar regime occurs for  $Ro_\ell$  closer to unity (see Figure 1).

The role of the local Rossby number in the dipolar-multipolar transition obviously relates to a dominant forces balance between inertial and Coriolis forces in the Navier-Stokes equation (1). This transition is associated with a breakdown of the dominant dipolarity of the dynamo as inertia increases, but it happens when inertial forces are still too small to suppress the columnar structure of convection. This subsequent hydrodynamic breakdown occurs at larger forcing and is discussed in *Soderlund et al.* [2013].

The transition between the dipolar regime and the multipolar regime is then expected to occur when the nongradient part of inertial forces is of the same order of magnitude as that of the Coriolis force. This statistical equilibrium can be expressed by considering the curl of this forces balance, it provides

$$\{\nabla \times (\mathbf{u} \times \nabla \times \mathbf{u})\} \sim \{\nabla \times (\mathbf{e}_z \times \mathbf{u})\}, \quad (6)$$

which can be rewritten as

$$\frac{u^2}{\ell \ell_u} \sim \frac{u}{\ell_{||}}. \quad (7)$$

Clearly  $\ell_u$ , as occurring in this relation, corresponds to the dissipation length scale defined in (5) and not to the often used  $\tilde{\ell}_u$ . In the following, we will thus only consider the length scale  $\ell_u$ . Below and at the transition, it is natural to assume  $\ell_{||} \sim 1$ . This implies

$$Ro_\ell \sim \ell, \quad (8)$$

where  $\ell$  is a nondimensional length scale which depends on correlations between the velocity and the vorticity. This length scale is thus an intricate quantity, which cannot be easily estimated a priori.

Note that assuming that  $\ell = 1$  is tantamount to writing the balance between inertial forces and the Coriolis force without taking the curl of each term.

#### 4. Coriolis Versus Viscous Forces

*King and Buffett* [2013] have shown that in numerical simulations, the typical length scale of the flow  $\tilde{\ell}_u$  verifies  $\tilde{\ell}_u \sim E^{1/3}$ . The scaling is even more naturally satisfied by the dissipation length scale  $\ell_u$ .

The  $E^{1/3}$ -scaling stems from the equilibrium between the nongradient part of the viscous force and the Coriolis force

$$\{E \nabla \times \nabla \times \nabla \times \mathbf{u}\} \sim \{\nabla \times (\mathbf{e}_z \times \mathbf{u})\}, \quad (9)$$

which provides

$$\frac{Eu}{\ell_u^3} \sim \frac{u}{\ell_{||}}. \quad (10)$$

This implies  $\ell_u \sim E^{1/3}$  which is well verified by dipolar dynamos ( $f_{\text{dip}} > 0.5$ ) in the database (see Figure 2).

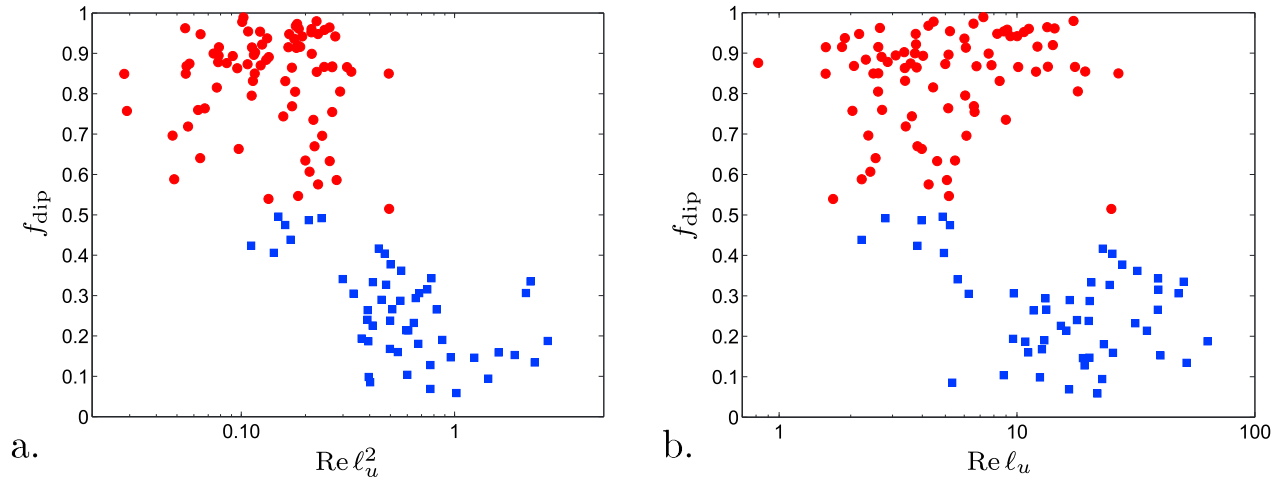


**Figure 3.** Dipolarity as measured by  $f_{\text{dip}}$  versus (a)  $Re \ell_u^2$  and (b)  $Re \ell_u$ . Red circles (respectively, blue squares) correspond to  $f_{\text{dip}} > 0.5$  (respectively,  $f_{\text{dip}} < 0.5$ ). These graphs rely on the 132 dynamos database. This figure stresses the importance of considering the curl of the forces balance in order to filter out the gradient parts in equilibrium with pressure forces.

### 5. Inertial Versus Viscous Forces

Because of this dominant balance between viscous forces and the Coriolis term, valid in the dipolar regime, the transition to multipolar dynamos necessarily also corresponds to a balance between inertial and viscous forces.

The statistical equilibrium between the nongradient part of inertial and viscous forces provides

$$\{\nabla \times (\mathbf{u} \times \nabla \times \mathbf{u})\} \sim \{E \nabla \times \nabla \times \nabla \times \mathbf{u}\}, \tag{11}$$

which can be rewritten as

$$\frac{u^2}{\ell \ell_u} \sim \frac{Eu}{\ell_u^3} \tag{12}$$

and corresponds to

$$Re \ell_u^2 \sim \ell, \tag{13}$$

where  $Re$  is the Reynolds number ( $Re \equiv RoE^{-1}$ ). Figure 3a supports the above relation. It is interesting to note that the parameter on the left of (13) is not the local Reynolds number ( $Re \ell_u$ ). Relation (13) relies on the curl of the forces balance, and contrasts with a transition corresponding to a simple balance between inertial and viscous forces. Such a naive balance would not filter the gradient parts and would yield the local Reynolds number  $Re \ell_u$  as relevant parameter. Such a scenario is obviously not supported by the numerical database (see Figure 3.b). Taking the curl of the Navier-Stokes equation (1) is therefore necessary before writing balances between these forces, in order to filter out the gradient part of the dominant forces.

### 6. A Three Forces Balance

It is quite clear from the above discussion that the transition between dipolar and multipolar dynamos occurs when the curl of inertial forces becomes comparable to both the curl of the Coriolis and of the viscous term, which were both in balance in the dipolar regime. As the Rayleigh number is increased, the role of inertia becomes more and more important, until the three forces balance is reached.

Indeed, replacing  $\ell_u$  by  $E^{1/3}$  in (8) and (13) yields the sole relation

$$Ro E^{-1/3} \equiv Re E^{2/3} \sim \ell. \tag{14}$$

This expression reveals the existence of a single parameter to describe the transition. We represent the dipolarity as a function of this parameter in Figure 4. This parameter provides a remarkable description

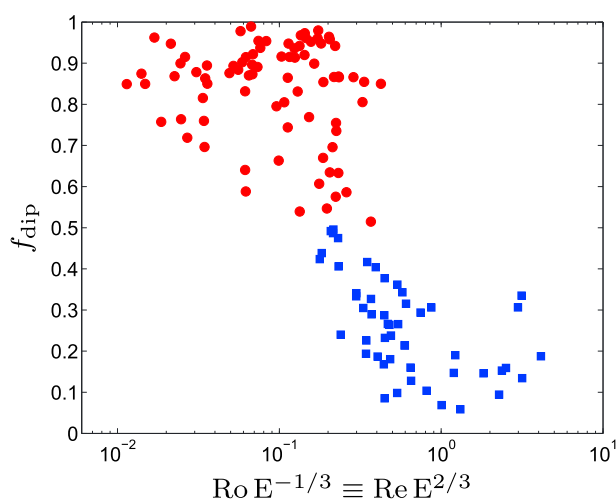


**Figure 4.** Dipolarity as measured by  $f_{\text{dip}}$  versus the sole parameter  $Ro E^{-1/3} \equiv Re E^{2/3}$ , revealing the three forces balance at the transition. Red circles (respectively, blue squares) correspond to  $f_{\text{dip}} > 0.5$  (respectively,  $f_{\text{dip}} < 0.5$ ). This figure relies on the 132 dynamos database.

estimate of the parameter  $Ro E^{-1/3} \equiv Re E^{2/3}$  then provides a typical value of  $10^{-1}$ . This is in agreement with the previous work of *Christensen* [2010], which argued that the Earth’s core would lie below, but close to the dipolar-multipolar transition. The vicinity to the critical value for transition to the multipolar state has been argued to be a possible reason for reversals of the Earth’s magnetic field [*Christensen*, 2010; *Wicht and Tilgner*, 2010].

It is important to note, however, that the resulting viscous length scale would be extremely small, less than 100 m. It is difficult to imagine that quasi-geostrophic structures would be stable in the Earth’s core on such small length scales. The viscous balance advocated here is usually ruled out for the Earth’s core, for which a magnetostrophic balance (between the nongradient part of the Coriolis and the Lorentz terms) is sought (see for a detailed discussion *Oruba and Dormy* [2014]). According to Figure 4, such models extended to the Earth’s core would produce a dynamo dominated by a strong dipole, yet close enough to the multipolar region to exhibit reversals [see also *Christensen*, 2010]. Presently available numerical models, however, appear to rely on a dominant forces balance, involving viscous forces, which is not relevant to the Earth’s core. Magnetostrophic numerical models still need to be produced.

### 8. Conclusions

We offer a unified description of the dominant forces balances at work in numerical dynamos and of the transition between the regime of steady dipolar dynamos and that of multipolar fluctuating dynamos. We show that it corresponds to a balance between three forces, i.e., the nongradient part of inertial, viscous, and Coriolis forces. This balance can be estimated by taking the curl of the dominant forces. We derive from this three terms equilibrium the parameter  $Ro E^{-1/3} \equiv Re E^{2/3}$  which provides an accurate description of the transition.

Using a measured length scale in the numerical models, the transition can be equivalently described by  $Ro/\ell_u$  (respectively,  $Re \ell_u^2$ ), which correspond to the two forces balance between the nongradient part of inertial (respectively, viscous) and Coriolis forces. The transition occurs when these parameters are order one, i.e., the forces are of comparable amplitude.

A more accurate description of the transition would require the knowledge of the correlation length scale  $\ell$  which is complex to determine. Figure 4 indicates that this nondimensional length scale is of order unity in the numerical database used in our study. It may be a function of other parameters (e.g., the Prandtl number  $Pr$  which is kept constant here). Further analysis of this correlation length scale in direct numerical simulations could provide a finer description for the transition.

of the transition. This vindicates the above scenario with a dominant balance between three terms at the transition, that is the nongradient part of inertial, viscous, and Coriolis forces.

### 7. The Geodynamo

It is important to ponder on the applicability of the above transition to the Earth’s core, as this can shed light on the relevance of available numerical models to geophysical observations. We use the typical estimates for the Earth’s core  $E = 10^{-14}$  [*Olson*, 2007] and  $Ro = 3 \times 10^{-6}$ , which corresponds to a typical RMS velocity in the core of  $1 \text{ mm s}^{-1}$  (order of magnitude obtained by inverting secular variation data) [see *Bloxham et al.*, 1989; *Christensen and Aubert*, 2006]. A direct

### Acknowledgments

The authors wish to thank Ludovic Petitdemange, Jonathan Aurnou, and Krista Soderlund for stimulating discussions. The database used in this work was kindly provided by Pr. U. Christensen (christensen@mps.mpg.de).

Michael Wysession thanks two anonymous reviewers for their assistance in evaluating this paper.

### References

- Bloxham, J., D. Gubbins, and A. Jackson (1989), Geomagnetic secular variation, *Philos. Trans. R. Soc. London*, 329, 415–502.
- Christensen, U. R. (2010), Dynamo scaling laws and applications to the planets, *Space Sci. Rev.*, 152, 565–590.
- Christensen, U. R., and J. Aubert (2006), Scaling properties of convection-driven dynamos in rotating spherical shells and application to planetary magnetic fields, *Geophys. J. Int.*, 166, 97–114.
- King, E. M., and B. A. Buffett (2013), Flow speeds and length scales in geodynamo models: The role of viscosity, *Earth Planet. Sci. Lett.*, 371–372, 156–162.
- Kuzner, C., and U. R. Christensen (2002), From stable dipolar towards reversing numerical dynamos, *Phys. Earth Planet. Inter.*, 131, 29–45.
- Olson, P. (2007), *Overview of Core Dynamics*, Treatise on Geophysics, vol. 8, Elsevier Science Publishers, Amsterdam.
- Oruba, L., and E. Dormy (2014), Predictive scaling laws for spherical rotating dynamos, *Geophys. J. Int.*, 198(2), 828–847, doi:10.1093/gji/ggu159.
- Schrinner, M., L. Petitdemange, and E. Dormy (2012), Dipole collapse and dynamo waves in global direct numerical simulations, *Astrophys. J.*, 752, 121.
- Soderlund, K. M., E. M. King, and J. M. Aurnou (2012), The influence of magnetic fields in planetary dynamo models, *Earth Planet. Sci. Lett.*, 333–334, 9–20.
- Soderlund, K. M., M. H. Heimpel, E. M. King, and J. M. Aurnou (2013), Turbulent models of ice giant internal dynamics: Dynamos, heat transfer, and zonal flows, *Icarus*, 224, 97–113.
- Wicht, J., and A. Tilgner (2010), Theory and modeling of planetary dynamos, *Space Sci. Rev.*, 152, 501–542.